International Journal of Automotive Technology, Vol. 7, No. 2, pp. 139–143 (2006)

1229-9138/2006/026-03

FLOW AND TEMPERATURE ANALYSIS WITHIN AUTOMOBILE CABIN BY DISCHARGED HOT AIR FROM DEFROST NOZZLE

W. G. PARK[1)*], M. S. PARK[1)] and K. L. JANG[2)]

[1)]School of Mechanical Engineering, Pusan National University, Busan 609-735, Korea
[2)]Test Team 3, R&D Division for HMC and KMC, 772-1 Jangduck-dong, Hwaseong-si, Gyeonggi 445-706, Korea

(Received 23 April 2004; Revised 23 December 2004)

ABSTRACT–As an automobile tends to be high grade, the needs for more luxurious interior and comfortable HVAC system are emerged. The defrosting ability is another major factor of the performances of HVAC system. The present work is to simulate the flow and the temperature field of cabin interior during the defrost mode. The three-dimensional incompressible Navier-Stokes equations and energy equation were solved on the multiblocked grid system by the iterative time marching method and AF scheme, respectively. The present computations were validated by the comparison of the temperature field of a driven cavity and velocity field of 1/5 model scale of an automobile. Generally good agreements were obtained. By the present computation, the complicated features of flow and temperature within the automotive cabin interior could be well understood.

KEY WORDS : Automobile cabin, Flow field, Temperature field, Navier-stokes equation, Energy equation

1. INTRODUCTION

As an automobile tends to be high grade, the demands for more luxurious interior and comfortable HVAC system are emerged. To satisfy these demands, the flow field analysis of a cabin interior should be preceded and, also, temperature field by hot air discharged from defrost nozzle should be accurately analyzed. Besides the comfortableness of HVAC system, the defrosting ability is another major factor of the performances of HVAC system. The safety regulation (SAE Standards, 1999) requires that, in the circumstances of –18°C of ambient temperature, the frost should be melted in 30 minutes in the defrosting mode by amount of more than 80% in zone-A and 100% in zone-C of Figure 1 after the engine starts. To test whether the defrosting system satisfies this safety regulation, a designer has been commonly accounting on experiments. However, as the computer and numerical algorithms make progress, the design has been gradually relying on CFD. Lee *et al.* (1994) used the commercial code, ICEM-CFD. Brewster *et al.* (1997) and AbdulNour (1998) used STAR-CD. Aroussi *et al.* (2001) used FLUENT to simulate velocity and temperature field on the wind glass. Komoriya *et al.* (1991) and Hur and Cho (1993) solved the flow field of vehicle passenger compartment.

*Corresponding author. e-mail: wgpark@pusan.ac.kr

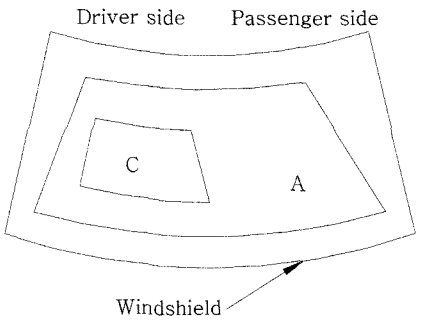

Figure 1. Indication of zones for safety regulation.

The objective of the present work is to simulate the flow and temperature field of the interior of an automobile cabin when the hot air is discharged from the defrost nozzle to melt the frost on the windshield glass.

2. GOVERNING EQUATIONS AND NUMERICAL METHODS

To obtain the flow field of a cabin interior, the 3-D incompressible Navier-Stokes equations are solved using the iterative time marching method (Park and Sankar, 1993; Park *et al.*, 2001).

$$\frac{\partial \hat{q}}{\partial \tau} + \frac{\partial(\hat{E} - \hat{E}_v)}{\partial \xi} + \frac{\partial(\hat{F} - \hat{F}_v)}{\partial \eta} + \frac{\partial(\hat{G} - \hat{G}_v)}{\partial \zeta} = 0 \qquad (1)$$

where $\hat{q} = [0, u, v, w]/J$. $\hat{E}$, $\hat{F}$, and $\hat{G}$ are the convective flux terms. $\hat{E}_v$, $\hat{F}_v$ and $\hat{G}_v$ are viscous flux terms. In the iterative time marching method, the continuity equation is solved by MAC method (Viecelli, 1969) and the momentum equation is solved by time marching scheme. The spatial derivatives of convective flux terms are differenced with QUICK scheme (Leonard, 1979). The spatial derivatives of viscous terms and continuity equation are differenced by the central differencing. To capture the turbulent flows, low Reynolds number k-ε model (Chien, 1982) was implemented. The detail description of numerical method is recommended to refer the paper of Park *et al.* (2001).

The temperature field is obtained from the incompressible energy equation.

$$\rho c_v \frac{\partial T}{\partial t} + \rho c_v \vec{V} \cdot \nabla T = \nabla \cdot (k \nabla T) \tag{2}$$

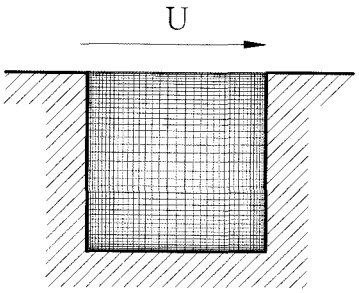

Figure 2. Grid of the driven cavity.

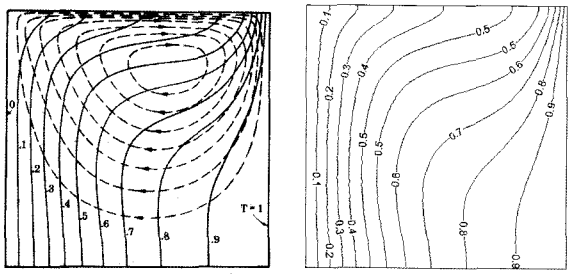

(a) Leonard (b) Present

Figure 3. Isotherms at Peclet number of 50.

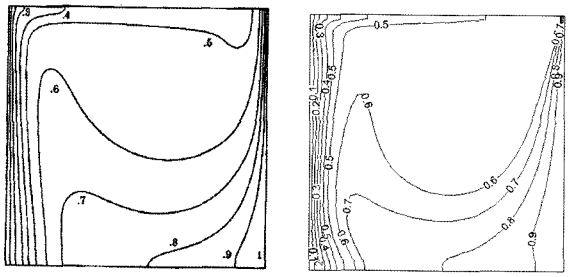

(a) Leonard (b) Present

Figure 4. Isotherms at Peclet number of 1,000.

where c_v, $\vec{V}$, and k are constant-volume specific heat, velocity vector, and coefficient of thermal conductivity, respectively. Since the energy equation is uncoupled with Navier-Stokes equations, the temperature field could be easily obtained by the time marching AF scheme, after is $\vec{V}$ obtained from equation (1).

3. RESULTS AND DISCUSSION

3.1. Code Validation

Since the iterative time marching method for solving

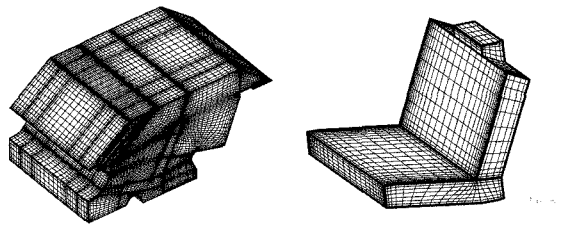

(a) Cabin (b) Chair

Figure 5. Grid system of 1/5 scale model of an automobile.

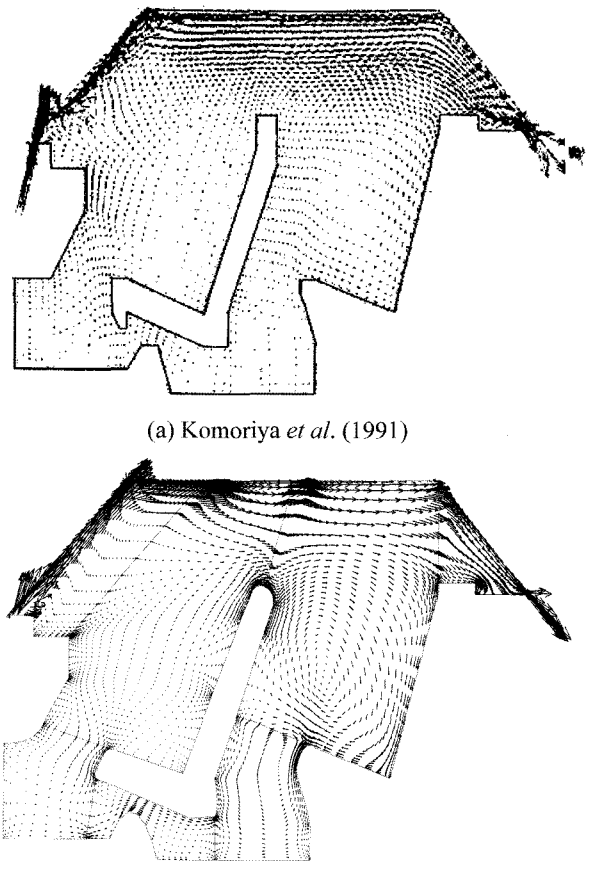

(a) Komoriya *et al.* (1991)

(b) Present

Figure 6. Velocity profiles of the cabin interior.

equation (1) has been thoroughly examined its validation for numerous internal and external flows (Park and Sanker, 1993; Park *et al.*, 2001; Jung *et al.*, 1998), the validation of numerical subroutine for energy equation is carried out in the present work. For this purpose, the driven cavity of Figure 2 was performed at Peclet number of 50 and 1,000 on the grid of 41 × 41. Figure 3 and 4 show the isotherms, compared with other numerical results (Leonard, 1979). Fairly good agreements are shown in these figures.

The interior flow of a cabin has been solved by the present method and compared with other numerical result. Figure 5 shows the grid for 1/5 scale model of an automobile, previously simulated by Komoriya *et al.* (1991). Total grid points are 730,000 with 13 multiblocks.

Figure 6 shows the velocity profiles, compared with numerical result of Komoriya *et al.* This figure also shows good agreement with each other. The cpu time was taken about 75 hours on the workstation that has Alpha-21264A processor (clock speed = 667 MHz). The general features of flow filed will be explained in section 3.2.

3.2. Flow and Temperature Analysis of Cabin Interior

Figure 7 shows the interior grid system of the automobile, which has been presently manufacturing and selling by an automobile company of Korea. The total grid points are about 4.8×10^6, consisted of 20 structured multiblocks.

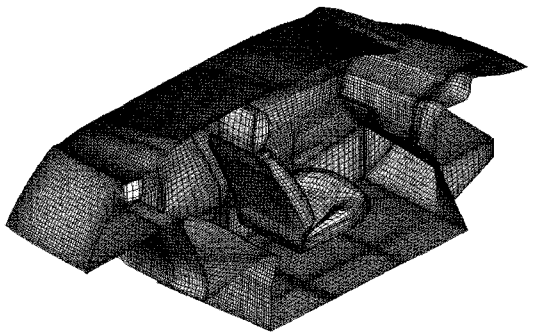

Figure 7. Grid system within the cabin of automobile.

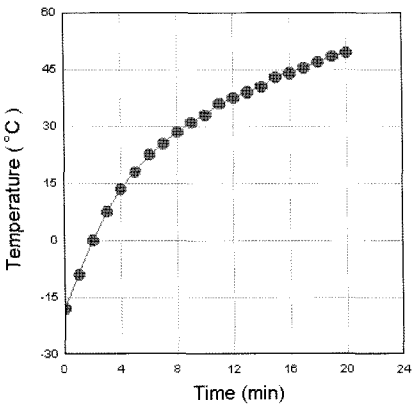

Figure 8. Time variation of temperature of discharged air.

Figure 8 shows the time history of the discharged air temperature measured at the exit of defrost nozzle after the engine starts up. The temperature of discharged air, initially at ambient temperature of −18°C, increases quite rapidly up to 50°C after 20 minutes.

Figure 9 shows velocity vectors on the windshield

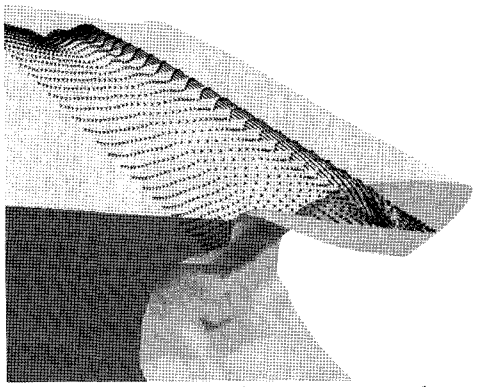

(a) Velocity vector in the symmetry plane

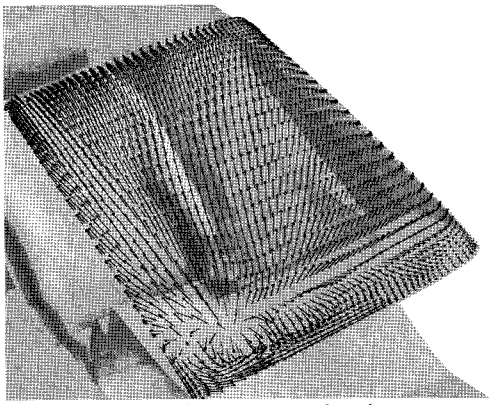

(b) Velocity vector on the glass

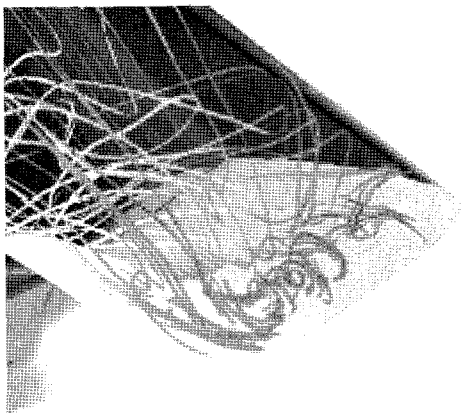

(c) Streamlines

Figure 9. Flow field near the windshield glass.

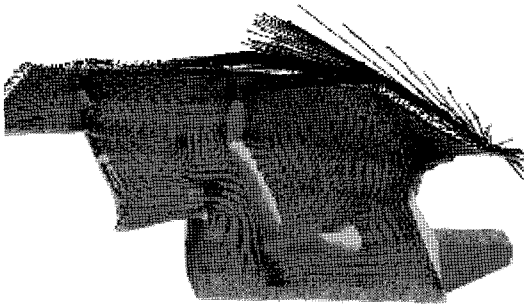

(a) In the plane of symmetry

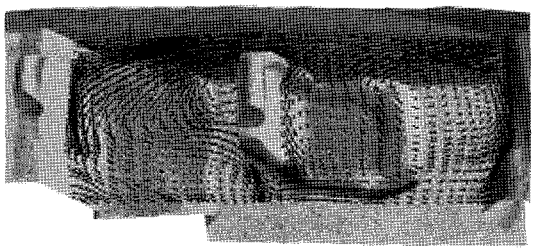

(b) In the plane of mid-height

Figure 10. Velocity vectors of the cabin interior.

glass and streamlines emanating from the defrost nozzle. Figure 9(a) shows the velocity vectors in the symmetry plane of the glass. In Figure 9(b), two significant strong flows are shown along the vertical direction near the center and diagonal direction. These strong flows dominantly affect the pattern of the defrosting propagation. Figure 9(c) gives the streamlines, showing strong diagonal flow and strong recirculating corner flow just above the instrument panel.

Figure 10 shows velocity vectors in the plane of symmetry and in the plane of mid-height of the cabin. In Figure 10(a), the strongly discharged air from the defrost nozzle flows along the windshield glass and, then, deflects its direction at the ceiling. Then, this flow expands its strength to the rear seat and also makes the recirculating flow in the upper region of front and rear seat. In the lower region of rear seat, the air flows downward and moves forward through the gap of the front seat. In the front seat region, the strong entrainment into the discharged air-jet is also shown. In Figure 10(b), it is shown that the diagonally discharged air, as shown in Figure 9(a), deflects its direction at the side wall of the cabin and, then, forms the recirculating flows after hitting the front and rear seat.

Figure 11 shows the streamlines that could explain the complicated flow features within the cabin. Figure 12 shows temperature contours in Kelvin (K) at 10 minutes in the defrost mode after the engine started. As expected, high temperature gradients occur near the glass in Figure 12(a). These high temperature gradients result in high

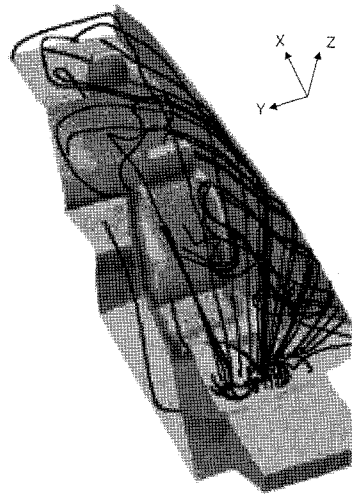

Figure 11. Streamlines in the cabin.

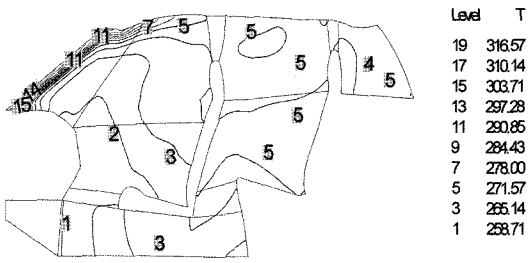

(a) In the plane of symmetry

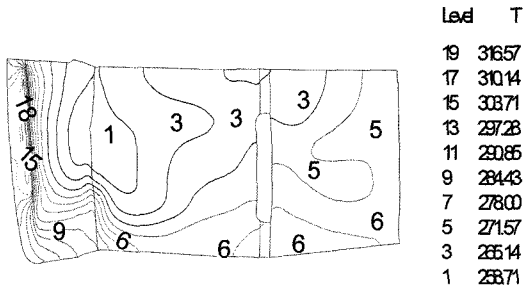

(b) In the plane of mid-height

Figure 12. Temperature contours of the cabin interior.

heat transfer across the windshield glass and provide thermal energy to the frost for melting. Since, as shown in Figure 10(a), the discharged hot air mainly flows along the ceiling during the defrost mode, the temperature of upper region is high than that of lower region. Also, the region of the rear seat is warmer than that of the front seat during the defrost mode because the discharged air dominantly flows first toward rear seat and, then flows forward to the front seat through the beneath of the front seat, as shown in Figure 10(a). From Figure 12(a), it is found that the lowest temperature region in the defrost

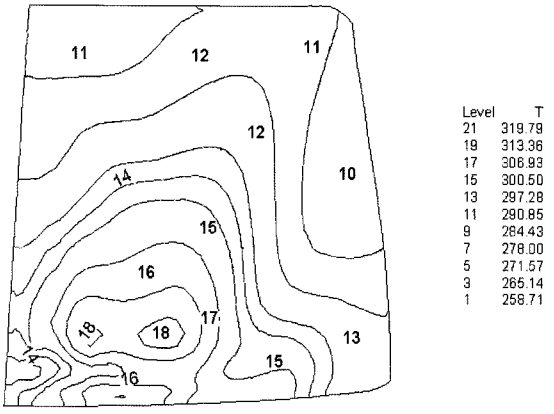

Figure 13. Temperature field on the windshield glass.

mode is the foot location of the driver. In Figure 12(b), besides high temperature field near the glass, another high temperature region is shown in the fore part of side wall. This is due to the discharged hot air which comes from the side exit of defrost nozzle to melt the frost of side window.

Figure 13 shows the temperature field on the windshield glass at 20 minutes. The strong diagonal flow, as shown in Figure 9(b), generates the high temperature field along the diagonal direction. From this figure, it is expected that the defrosting pattern will be propagated alog this diagonal direction.

4. CONCLUSION

To simulate the flow and the temperature field of cabin interior when the hot air is discharged from defrost nozzle, the three-dimensional incompressible Navier-Stokes equations and energy equation were solved on the multiblocked grid system. The present code was validated by the comparison of the temperature field of a driven cavity and velocity field of 1/5 model scale of an automobile. Generally good agreements were obtained. From the calculation of real automobile, the strong discharged air from the defrost nozzle flows along the windshield glass and deflects backward at the ceiling. Then, this flow makes the recirculating flow in the upper region of front and rear seat. In the rear seat, the air flows downward and moves forward through the gap of the front seat and, then, entrains into nozzle jet. The temperature field in the defrost mode indicates that high temperature gradient occurs near the windshield glass and relatively high temperature near the ceiling. The lowest temperature was found at foot location of the driver. The high temperature was shown along the diagonal direction of the glass. By the present simulation, the complicated flow and temperature features of automotive cabin interior could be well understood.

ACKNOWLEDGEMENT–This work was supported by BK21-project of Ministry of Education and Human Resources Development, Korea.

REFERENCES

AbdulNour, B. S. (1998). Numerical simulation of vehicle defrost flow field. *SAE Paper No.* 980285.

Aroussi, A., Hassan, A. and AbdulNour, B. S. (2001). Effects of vehicle windshield defrosting and demisting process on passenger comfort. *SAE Paper No.* 2001-01-1729.

Brewster, R. A., Frik, S. and Werner, F. (1997). Computational analysis of automotive windshield de-icing with comparison to test data. *SAE Paper No.* 971833.

Chien, K. Y. (1982). Predictions of change and boundary-layer flows with a low-reynolds number turbulence model. *AIAA J.* **20**, 33–38.

Hur, N. G. and Cho, W. K. (1993). 3-D numerical simulation of flows inside a passenger compartment of a model vehicle for hearting, air-conditioning and defrosting modes. *Trans. Korean Society of Automotive Engineers* **1**, **2**, 60–68.

Jung, Y. R., Park, W. G. and Ha, S. D. (1998). Numerical viscous flow analysis around a high speed train with crosswind effects. *AIAA J.* **36**, **3**, 477–479.

Komoriya, T., Kobayashi, T. and Taniguchi, N. (1991). Numerical simulation of the flow in a vehicle passenger compartment using general coordinate system with finite volume method. *Japan Society of Automotive Engineers Review* **12, 3,** 36–41.

Lee, J. G., Jiang, Y., Przekwas, J. and Sioshanasi, M. (1994). Validation of computational vehicle windshield de-icing process. *SAE Paper No.* 940600.

Leonard, B. P. (1979). A stable and accurate convective modeling procedure based on quadratic upstream interpolation. *Computational Methods in Applied Mechanics and Engineering*, **19**, 59–98.

Park, W. G. and Sankar, L. N. (1993). A technique for the prediction of unsteady incompressible viscous flows. *AIAA Paper* 93-3006.

Park, W. G., Taniguchi, N. and Kobayashi, T. (2001). Numerical flow analysis of generic body of car with cross-wind effect. *Proc. Japan Society of Automobile Engineers, JSAE Paper No.* 20015269, 17–20.

SAE Standards (1999). *Passenger Car Windshield Wipe Systems*. No. J903-C.

Viecelli, J. A. (1969). A method for including arbitrary external boundaries in the mac incompressible fluid computing technique. *J. Computational Physics*, **4**, 543–551.